

Eigenstates and excitations of the simple atom-molecule Bose-Einstein condensate

Marijan Koštrun and Juha Javanainen

*Department of Physics, University of Connecticut, Storrs, Connecticut 06269-3046 **

(Dated: May 22, 2019)

We analyze the mean-field eigenstates of the atom-molecule Bose-Einstein condensate (AMBEC) under the assumption that the background (elastic) scattering length of the atoms can be ignored. It is shown that the relevant eigenstates are localized in the space of the condensate parameters: The eigenstate has a different character in different regions of the parameter space, and at the interface of two local eigenstates the properties of the system may change nonanalytically. Using both analytical and numerical techniques, we find the approximate boundaries of the local eigenstates and identify the types of parametric excitations that occur when an eigenstate is forced outside of its region of validity by a parameter sweep. We contrast the properties of the mean-field parametric excitations found in AMBEC with the experimentally observed excitations of the BEC.

PACS numbers: 03.75.F,05.30.J,34.50

I. INTRODUCTION

The dynamics of the dilute, trapped Bose-Einstein condensates (BEC) of a single atomic species has been successfully modeled using the Gross-Pitaevskii equation (GPE) [1, 2] [toss these reference],

$$i\hbar \frac{\partial \Phi(\mathbf{r}, t)}{\partial t} = \left(-\frac{\hbar^2}{2m} \nabla^2 + V_0(\mathbf{r}, t) \right) \Phi(\mathbf{r}, t) + \frac{4\pi \hbar^2 a N}{m} |\Phi(\mathbf{r}, t)|^2 \Phi(\mathbf{r}, t). \quad (1)$$

Here Φ is the mean-field amplitude of the atomic condensate, normalized to unity, N is the number of atoms in the condensate, m is the mass of an atom, V_0 is the trapping potential, and a is the atom-atom s-wave scattering length. The properties of the mean-field ground state Φ of Eq.(1) depend on the sign of a . If $a > 0$ the ground state Φ is a single, well behaved function. However, when $a < 0$, there may be two solutions: the ground state, which is the collapsed state of the condensate represented by a δ -function, and a metastable state, which acts as a continuation of the positive- a ground state to the negative values of a . The metastable eigenstate exists only for limited values of the parameters $N a/\ell \gtrsim -0.67$, where ℓ is the characteristic length of the harmonic trapping potential V_0 . If $N a/\ell$ is driven beyond this limit by increasing, say, the atom number in the condensate, the amplitude Φ collapses [3–7]. It has been argued that the collapse in the BEC takes a finite time [8] and leads to a gas-liquid phase transition [9–11].

Controlling the collapse is but one motivation for the current flurry of effort toward controlling the scattering length [6, 12–14]. Generally, atom-atom interactions can be manipulated experimentally by adjusting the coupling of a pair of atoms to the corresponding molecular dimer with a static magnetic field (Feshbach resonance)

or with electromagnetic radiation (photoassociation) [15–19]. [add Stwalley’s suggestion]. These schemes may be modeled with a quantum field theory of coupled atomic and molecular fields. A formally identical field theory can be devised for elastic resonant scattering [20], with the difference that the scattering resonances takes the role of the molecular dimer. All of these approaches lead to the same mean-field theory of the atom-molecule BEC (AMBEC) in which there are three parameters: K , coupling strength between pairs of atoms and molecules; δ , detuning of the molecular state from the edge of the two-atom continuum; and a_{bg} , background atom-atom scattering length.

In this paper we examine the eigenstates of the mean-field AMBEC under the simplifying assumption that $a_{bg} = 0$. The focus is on two eigenstates: the thermodynamically stable ground state, and a “twin” state that, we believe, is often more relevant than the ground state in experiments starting with an atomic condensate. Using numerical and analytical techniques we show that the $\{\delta, K\}$ parameter space is divided into regions, between which the nature of the eigenstate abruptly changes. We associate the existence of such “local” eigenstates within a “global” eigenstate with the non-linearity of the mean-field theory of the coupling between the atoms and the molecules.

When the system is created in a local eigenstate and is subsequently pushed by a time-dependent variation of the parameters into a region in which the initial local eigenstate no longer exists, parametric excitations ensue. We will characterize and classify the excitation analytically and numerically.

Finally, we will point out intriguing similarities with experiments. Caution is due in such comparisons, as the motion of the atoms and the molecules in the trap is significant in our calculations and not necessarily so in all experiments. Conversely, though, in genuine trap experiments heretofore unrecognized possibilities open up. In particular, with a proper variation of the parameters the collapse of a condensate with a negative (effective) scattering length may be achieved continuously and in a

*Electronic address: kostrun@phys.uconn.edu; URL: <http://krampus.phys.uconn.edu>

controllable fashion.

II. MEAN FIELD MODEL OF SIMPLE AMBEC

We use the mean fields φ and ψ to describe atomic and molecular condensates, respectively. The interaction energy produced by the coupling between the condensates reads

$$E_I = -\frac{1}{2}K (\langle \varphi^2 | \psi \rangle + \langle \psi | \varphi^2 \rangle). \quad (2)$$

In the theory of Feshbach resonances, K^2 is proportional to the width of the resonance [21–24]. Conversely, in photoassociation, K^2 is a controllable parameter proportional to laser intensity [18].

Our assumptions of the simple AMBEC lead to the following set of scaled coupled Gross-Pitaevskii equations,

$$i \frac{\partial \varphi}{\partial \tau} = H_a \varphi - K \varphi^* \psi, \quad (3a)$$

$$i \frac{\partial \psi}{\partial \tau} = (H_m - \delta) \psi - K \varphi^2. \quad (3b)$$

The detuning δ measures the difference in energy of an atomic pair and the discrete molecular state. Here we choose the sign of δ so that a positive (negative) detuning produces a positive (negative) effective scattering length. The Hamiltonians H_a and H_m correspond to the center-of-mass energies for atoms and molecules, respectively,

$$H_a = -\frac{1}{2} \nabla^2 + \frac{1}{2} \sum_i \omega_{a,i}^2 x_i^2, \quad (4a)$$

$$H_m = -\frac{1}{4} \nabla^2 + \sum_i \omega_{m,i}^2 x_i^2. \quad (4b)$$

For simplicity, we assume that the trap is isotropic with $\omega = 1$. Lastly, we scale the fields so that the normalization reads

$$\langle \varphi | \varphi \rangle + \langle \psi | \psi \rangle = 1. \quad (5)$$

The expression for the conserved total energy of the system is then

$$E = \langle \varphi | H_a | \varphi \rangle + \frac{1}{2} \langle \psi | H_m - \delta | \psi \rangle + E_I. \quad (6)$$

There are numerous practical issues with the model embodied in Eqs. (3), many of which have been discussed elsewhere, e.g., in Ref. [18]. Here we focus on the AMBEC eigenstates, either global (stretching over the whole parameter space) or local (limited to certain regions of the parameter space), an important issue of principle associated with variations of the AMBEC parameters δ and K . For the most part, we ignore the complications of real experiments.

III. EIGENSTATES OF ZERO-DIMENSIONAL AMBEC: GROUND STATE AND TWIN STATE

The system of GPE (3) of a simple AMBEC is nonlinear in the amplitudes φ and ψ . For that reason we start our discussion of the AMBEC spectrum with an analysis of its simpler, zero-dimensional, version, and recite some elementary results [15, 18, 25].

A zero-dimensional AMBEC model is obtained by replacing the Hamiltonians H_a and H_m in (3) with constants, which are subsequently absorbed in δ . The time evolution of the atomic (α) and molecular (β) amplitudes is then governed by a system of ordinary differential equations (ODE),

$$i \dot{\alpha} = -K \alpha^* \beta, \quad (7a)$$

$$i \dot{\beta} = -\delta \beta - K \alpha^2. \quad (7b)$$

The stationary solutions are sought in the form $\alpha = x \cdot \exp(-i \mu t)$ and $\beta = y \cdot \exp(-i 2 \mu t)$. Additionally, the normalization (5) transforms into $x^2 + y^2 \equiv 1$.

We find three possible solutions: the ground state, the twin state and the all-molecule state. The all-molecule state is a trivial solution with the amplitude $y \equiv 1$ and the eigenenergy $\mu = -\bar{\delta}/2$, where $\bar{\delta} = \delta/K$. The ground state has the molecular amplitude

$$y_{GS}(\bar{\delta}) = \begin{cases} \frac{\bar{\delta}}{6} + \frac{\sqrt{\bar{\delta}^2 + 12}}{6}, & \text{for } \bar{\delta} \leq 2, \\ 1, & \text{for } \bar{\delta} > 2, \end{cases} \quad (8)$$

and the frequency is

$$\mu_{GS}(\bar{\delta}) = \begin{cases} -\frac{\bar{\delta}}{6} - \frac{\sqrt{\bar{\delta}^2 + 12}}{6}, & \text{for } \bar{\delta} \leq 2, \\ -\frac{\bar{\delta}}{2}, & \text{for } \bar{\delta} > 2. \end{cases} \quad (9)$$

The twin state is specified by

$$y_{TW}(\bar{\delta}) = \begin{cases} -1, & \text{for } \bar{\delta} < -2, \\ \frac{\bar{\delta}}{6} - \frac{\sqrt{\bar{\delta}^2 + 12}}{6}, & \text{for } \bar{\delta} \geq 2, \end{cases} \quad (10)$$

with

$$\mu_{TW}(\bar{\delta}) = \begin{cases} \frac{\bar{\delta}}{2}, & \text{for } \bar{\delta} < -2, \\ -\frac{\bar{\delta}}{6} + \frac{\sqrt{\bar{\delta}^2 + 12}}{6}, & \text{for } \bar{\delta} \geq 2. \end{cases} \quad (11)$$

In terms of the fraction of atoms, the ground state (8) behaves as follows. For large negative detunings, $\bar{\delta} \ll -1$, the ground state consists almost entirely of atoms. The fraction of molecules increases as we approach $\bar{\delta}_c = 2$ from below. At the non-analytic point $\bar{\delta} = \bar{\delta}_c$ the ground state merges with the all-molecule state ($y \equiv 1$), but that merge is not smooth. The twin state (10) behaves similarly, as the ground and twin states transform between each other with the operations $\bar{\delta} \rightarrow -\bar{\delta}$ and $y \rightarrow -y$. For large positive detunings, $\bar{\delta} \gg K$, the fraction of atoms is almost unity and it decreases as we approach $\bar{\delta} = -2$ from above. At $\bar{\delta} = -\bar{\delta}_c$ the twin state merges with the

all-molecule state ($y \equiv -1$). However, as was the case with the ground state, the transition to an all-molecule state is continuous but not smooth.

We next examine the stability of the stationary solutions of Eq. (7) by finding their frequencies of small oscillations. The most convenient variables are the molecular amplitude y and the phase difference between the square of the atomic amplitude and the molecular amplitude, $\theta = 2 \arg(\varphi) - \arg(\psi)$. In these new variables the original system of ODE's (7) reads

$$\dot{y} = (1 - y^2) \sin \theta, \quad (12a)$$

$$\dot{\theta} = \bar{\delta} + \left(\frac{1}{y} - 3y \right) \cos \theta. \quad (12b)$$

Its nontrivial ($x \neq 0$) fixed points are constructed from the solutions (8) and (10) so that the amplitude y is positive. The ground state is then $y = y_{GS}$, (8), with phase $\theta = 0$. The twin state has the phase $\theta = \pi$ and consequently $y = -y_T$, (10). Both stationary solutions have the same frequency of small oscillations derived from

$$\Omega^2 = \cos^2 \theta (1 - y^2) \left(\frac{1}{y^2} + 3 \right), \quad (13)$$

which always gives a real number.

For the all-molecule solution the analysis is somewhat more complicated. For $|\bar{\delta}| < 2$ the all-molecule state is unstable [25], while for $|\bar{\delta}| > 2$ it is stable. To get a feel for how the stably the all-molecule state behaves, let us consider the large $\bar{\delta} = \delta/K$ limit and write the molecular amplitude as $y = 1 - \delta y$. In that limit the approximate solution for phase θ is $\theta \approx \bar{\delta} t$. Solving (12a) for $\delta y(t)$ yields

$$\delta y(t) \approx \delta y(0) \cdot \exp \left[-\frac{\sqrt{2}}{\bar{\delta}} (1 - \cos(\bar{\delta} t)) \right]. \quad (14)$$

That is, for $|\bar{\delta}| > 2$ the all-molecule solution is stable, but not an attractor: the oscillations of amplitudes in the vicinity of the all-molecule state are persistent and do not decay with time.

To conclude, the zero-dimensional model (7) has three stationary states: the ground state, the twin state and the all-molecule state. The ground state (twin state) has a non-analytic point at $\bar{\delta} = +2$ (-2) where it merges with the all-molecule state. A detuning sweep across either of the non-analytic points creates parametric excitations of the amplitudes, the details of which depend on the numerical details (sweep rate, initial conditions). Commonly, these excitations manifest themselves in small, persistent, non-linear oscillations near the all-molecule state.

IV. GROUND STATE AND TWIN STATE IN SIMPLE AMBEC - NUMERICAL STUDY

The simple AMBEC (3) inherits much of the behavior of the zero-dimensional version, but also adds some

unexpected twists. Before going into the details, we expand on some terminology we have already brought up in passing.

The zero-dimensional model has stationary states, or eigenstates. A notable one is the ground state, the eigenstate with the lowest chemical potential. There are no general criteria for the existence of eigenstates for non-linear differential operators, but it appears from our numerical calculations that the simple AMBEC, too, has a unique ground state for all parameters δ and K . As the ground state can be identified, seemingly unambiguously, in the entire parameter space, we call it a *global* eigenstate.

In the zero-dimensional model the nature of the ground state is different depending on the parameters. For instance, if $\bar{\delta} > 2$, the ground state is all molecules. A similar behavior is found in the ground state of the AMBEC. Locally, in different regions of the parameter space, the ground state may be (nearly) all molecules, (nearly) all atoms, or a mixture of atoms and molecules. As in the zero-dimensional case, the nature of the ground state may change nonanalytically when the AMBEC parameters are varied. We say that at such a point of nonanalyticity the global ground state of the AMBEC switches from one local (in the $\{\delta, K\}$ space) eigenstate to another. We characterize local eigenstates as all-atom, all-molecule, or mixed atom-molecule. On occasion, this distinction is qualitative only. For instance, the all-atom state may not be all atoms, but the fraction of atoms is much larger than in the adjacent mixed atom-molecule state.

However, the experiments do not always deal with the ground state. In a Feshbach resonant system, what seemingly is an atomic BEC may be prepared with parameters such that the ground state of the AMBEC would be all molecules. We introduce the *twin* state analogous of the twin state in the zero-dimensional case to model this type of a situation. We construct the twin state numerically by starting with an all-atom ground state of the noninteracting system ($K = 0$), and then vary K adiabatically. This procedure appears to produce an eigenstate of the AMBEC system for all $\delta > 0$ and K . It appears that for certain $K > 0$ and $\delta < 0$ the twin state is unstable, and in practice it is not possible to construct it numerically by integrating the AMBEC system in time. Nevertheless, we surmise that we have here another global eigenstate of the AMBEC. Just like the ground state, we expect the twin state to be split into three local eigenstates, : all-atom, all-molecule, and mixed atom-molecule eigenstate.

Except for stationary states, we will also investigate what happens when the parameters δ and K are varied in time. The general observation is that, where the system switches from one local eigenstate to another, various type parametric excitations set in.

The present Section IV reports on numerical studies about the breakdown of the ground state and the twin state into local eigenstates, and describes the parametric excitations that ensue when a parameter is swept across a border between local eigenstates.

A. Ground State

Here we calculate the ground state numerically. While the work in three dimensions is feasible in principle, the computations are restricted to spherically symmetric situations for simplicity. We employ the DS-method [26]. The iteration that is repeated until convergence consists of integration in complex time followed by the renormalization, see Appendix A. For a point (δ, K) in parameter space we find the solutions φ and ψ for the amplitudes. Next we determine the atomic fraction, which is the same as the norm of atomic amplitude, $N_a = \langle \varphi | \varphi \rangle$, and the half-size $R_{1/2}$, Eq. (A4), of the atomic distribution. The calculation of the ground state amplitudes is done over an integer mesh $\delta = -30 \dots 30$, and $K = 0.1, 1 \dots 30$; where we use $K = 0.1$ as an approximation of the limit $K \rightarrow 0$.

The fraction of the atoms and the half-size in the ground state are shown in Figs. 1 and 2, respectively, for different points in the $\{\delta, K\}$ parameter space. We observe that the ground state consists of three local eigenstates: all-atom state, mixed or atom-molecule state, and all-molecule state. We refer to the boundaries of particular eigenstate as a fractures, and label them as follows. The all-atom state is bounded by the fracture f_{GS}^1 from the mixed or atom-molecule state and similarly, the all-molecule eigenstate is bounded by the fracture f_{GS}^2 from the mixed or atom-molecule state.

We next demonstrate how a parameter sweep of the eigenstate across the fracture creates a parametric excitation. In the first example we perform an intensity sweep, with $K = 0 \dots 18$ and $\delta = -30$. The behavior of the atomic fraction and the half-size is shown in Fig. 3. As surmised, at the fracture f_{GS}^1 the local all-atom eigenstate disappears causing a parametric excitation of both amplitudes. The extent of the excitation is determined by the relative position of the mixed or atom-molecule eigenstate (which becomes a new ground state) and the numerical details of the sweep (rate, initial conditions).

In the second example we perform a positive detuning sweep, with $\delta = -30 \dots 30$ and $K = 10$. Fig. 4 shows the behavior of the norm and the half-size of the atomic distribution. For $\delta < 0$ we find no evidence for parametric excitations in the amplitudes, meaning that the all-atom state may continuously evolve into the mixed or atom-molecule state in some regions of parameter space. For $\delta > 0$, close to the fracture f_{GS}^2 , we observe another parametric excitation.

The parametric excitations at f_{GS}^2 and f_{GS}^1 differ. At f_{GS}^2 the oscillations of the atomic quantities are erratic, whereas at f_{GS}^1 the oscillations are periodic. We return to these differences in Sec. V, when we analyze the solutions for the amplitudes analytically.

B. Twin State

In the zero-dimensional model, the twin state and the ground state are related via the transformation $\delta \rightarrow -\delta, K \rightarrow -K$. Applying this transformation to the ground state, we surmise that the twin state contains the all-atom state for $\delta > 0, K \rightarrow 0$, and may include the all-molecule state.

We test our assumptions using numerical methods. For parameters $K > 0$ and $\delta > 0$, the twin state is prepared from the all-atom state, ground state of the atomic system in the given trap, by slowly varying the matrix element K from zero to the desired value at the fixed detuning δ . Following such an adiabatic preparation, the twin state is monitored in the standard fashion while one of the parameters, either the detuning δ or the matrix element K , is varied.

We limit the exposition of our results to two characteristic examples. In the first example, shown in Fig. 5, we fix the detuning at $\delta = 100$ and vary K in the range $0 \dots 36$. As can be seen, the fraction of the atoms stays close to 1 at all times, while the half-size of the atomic condensate increases slightly. We observe that there are no parametric excitations, and conclude that the all-atom state exists for $\delta > 0$ and $K > 0$. This reaffirms adiabatic intensity sweep as a method for preparing the twin state for positive detunings, and demonstrates the absence of the analogue of the ground state fracture f_{GS}^1 in the twin state.

In the second example we take the twin state prepared at $\delta = 50$ and $K = 10$, and perform a negative detuning sweep $\delta = 50 \dots -50$. The behavior of the norm and the half-size of the atomic distribution are shown in Fig. 6. For $\delta > 0$ the all-atom state has no parametric excitations, in accord with the first twin-state example. Around $\delta \approx 0$ the fraction of the molecules starts to increase and the all-atom eigenstate becomes a mixed or atom-molecule eigenstate with an increasing fraction of molecules. At some negative δ we find familiar signatures of a strong parametric excitation in the atomic quantities, which suddenly start to oscillate chaotically. We refer to the set of points in the $\{\delta, K\}$ parameter space where the parametric excitations set in as the fracture f_{TW} .

V. ANALYTIC BOUNDARIES OF LOCAL EIGENSTATES

Both the twin state and the ground state have as a local eigenstate either an all-molecule state (zero-fraction of atoms), or an all-atom state (negligible fraction of molecules). The boundaries of those two special eigenstates in the parameter space may be found using analytic methods. Our next task thus is to find analytic expressions for the boundaries of the local eigenstates. We also compare the results with direct numerical computations.

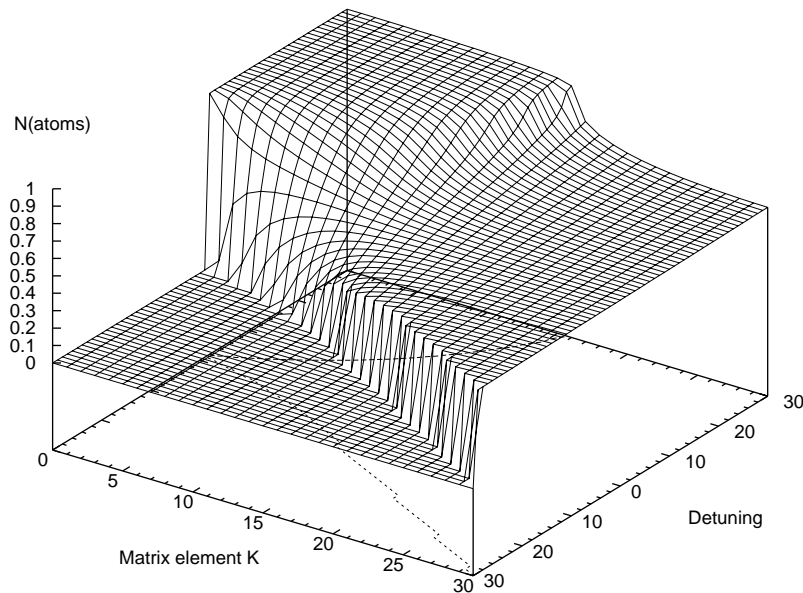


FIG. 1: Fraction of atoms (N_a) in the ground state as a function of the detuning δ and the atom-molecule coupling K .

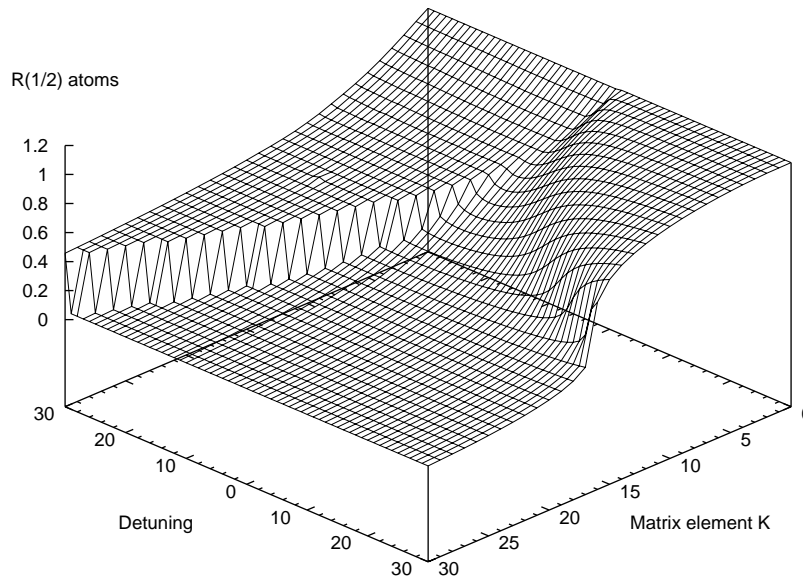


FIG. 2: Half-size $R_{1/2}$, Eq. (A4), of the atomic distribution in the ground state as a function of the detuning δ and the atom-molecule coupling K .

A. All-atom state; fracture f_{GS}^1

In the limit $K \rightarrow 0$ and $-\delta \gg K$ the fraction of molecules becomes negligible, so it is possible to eliminate the molecules from the theory. Performed in the standard way, this procedure leads to a single-condensate GPE with a negative scattering length. Its solution is either a single collapsed state or a pair consisting of the collapsed state and the “metastable” (non-collapsed) state. The collapse boundary in this approach is the boundary of the metastable state in the parameter space. In the variational approach [3] the collapse boundary is given by

$a_c \approx -0.67$, which in terms of the AMBEC parameters reads $\frac{K^2}{4\pi\delta} \approx -0.67$.

We observe that there is a contradiction between the “no-collapse” theorem [27], according to which the AMBEC amplitudes may not collapse, and the “standard” single-condensate approximation of the AMBEC, in which the collapse of the atomic amplitude is allowed. We resolve the contradiction by reexamining the effective scattering length expansion, and demonstrate that the usual expansion is incomplete. We recall that Eq. (3b)

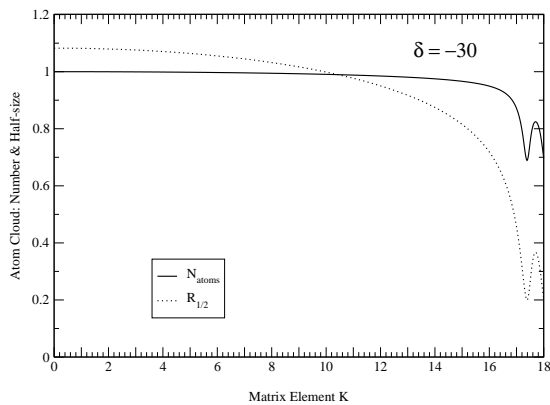


FIG. 3: (Ground State) Norm N_a and the half-size $R_{1/2}$ of the atomic distribution for the intensity sweep $K = 0 \dots 18$ with fixed $\delta = -30$. Integration is performed in 50,000 steps of size (A2). At f_{GS}^1 the atomic variables begin to oscillate.

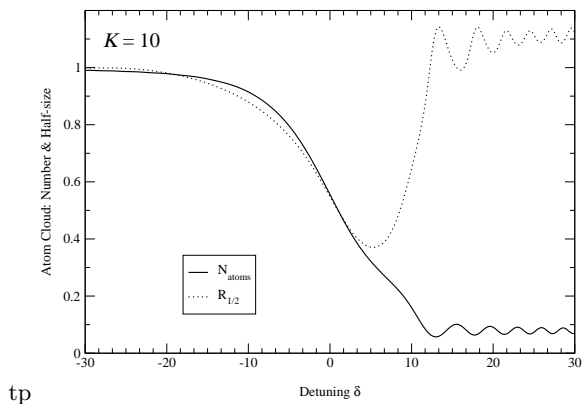


FIG. 4: (Ground State) Norm N_a and the half-size $R_{1/2}$ of the atomic distribution for the detuning sweep $\delta = -30 \dots 30$ with fixed $K = 10$, done in 50,000 steps of size (A2). Following f_{GS}^2 the half-size of the atomic condensate begins to oscillate erratically.

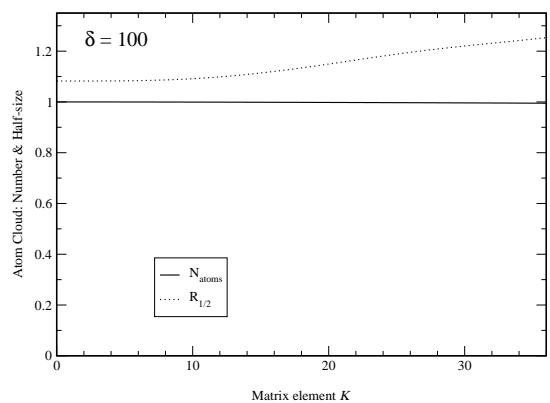


FIG. 5: (Twin State) Norm N_a and the half-size $R_{1/2}$ of the atomic distribution for the intensity sweep $K = 0 \dots 36$ with fixed $\delta = 100$, done in 150,000 steps of size (A2). We see no evidence of parametric excitations.

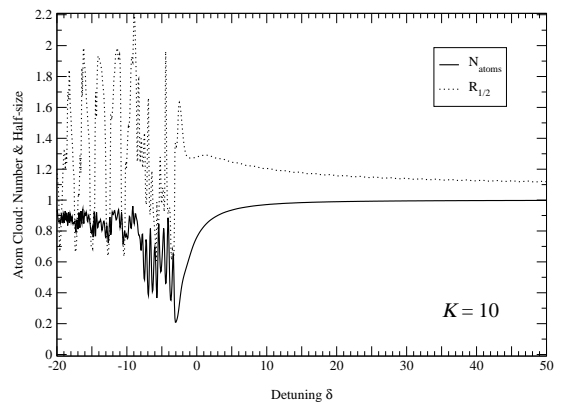


FIG. 6: (Twin State) Norm N_a and the half-size $R_{1/2}$ of the atomic condensate for the negative detuning sweep $\delta = 50 \dots -20$ with fixed $K = 10$, done in 100,000 steps of size (A2). The time is reversed (goes from right to left) so that the detuning axis has the same orientation as in Fig. 4. Following f_{TW} the molecules decay rapidly into atoms and both atomic and molecular distributions begin to oscillate erratically in half-size and fraction.

can be formally solved for the field ψ [27], yielding

$$\begin{aligned} \psi &= -K \left(i \frac{\partial}{\partial t} + \delta - H_m \right)^{-1} \varphi^2 \\ &= -\frac{K}{\delta} \sum_{j=0}^{\infty} \left[\frac{1}{\delta} \left(i \frac{\partial}{\partial t} - H_m \right) \right]^j \varphi^2. \end{aligned} \quad (15)$$

In the limit $N_m = \langle \psi | \psi \rangle \ll 1$ and large $|\delta|$, the term $i \frac{\partial \psi}{\partial t} \simeq 2\mu\psi \sim \frac{1}{\delta}\psi$ can be neglected in (15) when compared to $H_m\psi \sim \frac{3}{2}\psi$.

After removing the partial time derivative in (15), we group the terms with $j = 0$ and $j = 1$, then $j = 2$ and $j = 3$, and so forth. The new expansion is well behaved; if the amplitudes collapse for whatever reason, $\varphi(\mathbf{r}) \rightarrow \delta(\mathbf{r})$, each term in the rearranged expansion grows to $+\infty$. The δ -function is thus a solution with an infinite positive energy and the collapse of the condensate is not energetically favorable, in accord with the “no-collapse” theorem. The correct leading-order approximation for H'_a , which combines the terms $j = 0$ (effective scattering) and $j = 1$ (formation of a coherent atom pair), reads

$$H'_a \varphi = H_a \varphi + \frac{K^2}{\delta} |\varphi|^2 \varphi + \frac{K^2}{\delta^2} \varphi^{*2} H_m \varphi, \quad (16)$$

with H_a and H_m from Eqs. (4). We observe that in this approximation a molecule (a new entity made of two atoms) is replaced by a quasi-particle (a coherent excited state of two atoms).

We examine the eigenstates of the Hamiltonian H'_a using the variational approximation [15, 28, 29]. The total energy is given by

$$E_a(\varphi) = \langle \varphi | H_a | \varphi \rangle + \frac{K^2}{2\delta} \langle \varphi^2 | \varphi^2 \rangle + \frac{K^2}{2\delta^2} \langle \varphi^2 | H_m | \varphi^2 \rangle. \quad (17)$$

Here the atomic eigenstate φ is approximated by a Gaus-

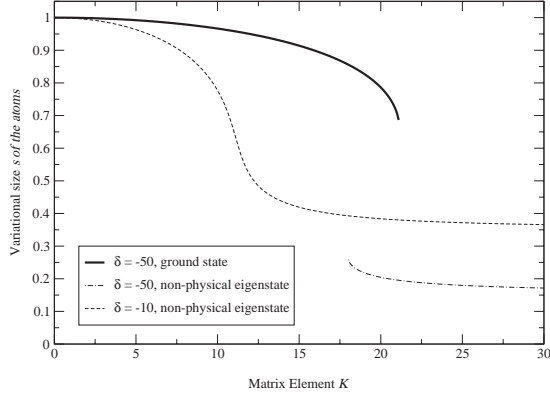


FIG. 7: Variational sizes of atomic distribution for the detunings $\delta = -10$ and $\delta = -50$, with $K = 0 \dots 30$. For $\delta = -10$, there is a single non-physical solution. For $\delta = -50$, there are two solutions, one of which is the ground state.

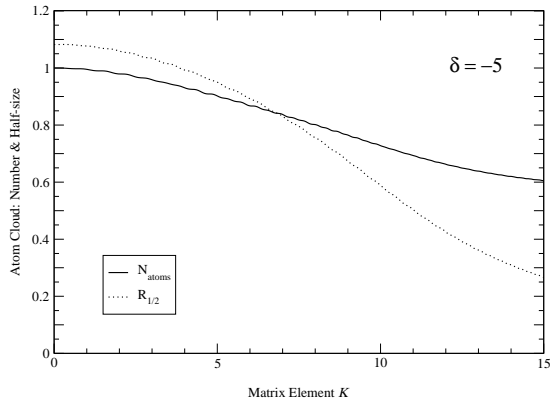


FIG. 8: Adiabatic evolution of the initial all-atom eigenstate at the fixed detuning $\delta = -5$ for $K = 0 \dots 15$, in terms of the fraction of atoms and the half-size of the atomic distribution.

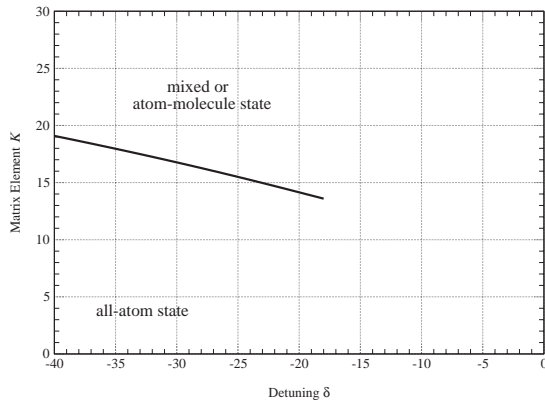


FIG. 9: The position of f_{GS}^1 in the parameter space, found using the variational approximation.

δ	K_{th}	K_{num}	N_a^{aa}	N_a^{mix}	$R_{1/2}^{aa}$	$R_{1/2}^{mix}$
-100	29.5	30.5 ± 0.5	0.99	0.52	0.98	0.05
-90	28	27.5 ± 0.5	0.99	0.54	0.78	0.07
-80	26.5	25.5 ± 0.5	0.99	0.56	0.84	0.08
-70	24.8	24.5 ± 0.5	0.98	0.57	0.74	0.09
-60	23.1	22.5 ± 0.5	0.98	0.59	0.80	0.11
-50	21.1	20.5 ± 0.5	0.98	0.62	0.81	0.14
-40	19.1	18.5 ± 0.5	0.97	0.66	0.81	0.18
-30	16.8	16.5 ± 0.5	0.96	0.70	0.82	0.24
-20	14.1	14.5 ± 0.5	0.92	0.73	0.69	0.33

TABLE I: Analytical (K_{th}) and numerical (K_{num}) positions of f_{GS}^1 in the parameter space. The atomic fraction (N_{aa}) and half-size of the atomic distribution ($R_{1/2}$) are evaluated numerically on the opposite sides of f_{GS}^1 : for the all-atom eigenstate at $K = K_{num} - 0.5$ (*aa*), and for the mixed or atom molecule state at $K = K_{num} + 0.5$ (*mix*).

sian depending on a single variational parameter s ,

$$\varphi_s(r) = \left(\frac{m\omega}{\pi s^2}\right)^{3/4} e^{-\frac{m\omega r^2}{2s^2}}. \quad (18)$$

The total energy becomes a function of the variational condensate size s . The variational eigenstates are the states of the form (18) for which the size s is a local minimum of the energy functional $E_a(s)$. That is, the variational sizes $\{s_i\}_{i=1\dots}$ are the real positive roots of $dE/ds(s_i) = 0$ such that $d^2E/ds^2(s_i) > 0$. We use MATHEMATICA[®] to find the solutions for the variational size of the atomic condensate, and keep only those solutions which do not exist in the limit $K \rightarrow \infty$ for a given $\delta < 0$. Our choice of a physical all-atom eigenstate is justified considering the behavior of the fraction of atoms in the ground state shown in Fig. 1. In the limit $K \rightarrow \infty$ the ground state is not an all-atom state. In this approximation, for given $\delta < 0$, the fracture f_{GS}^1 occurs at the value of K for which the all-atom ground state disappears.

To illustrate this point, let us consider the variational size for two fixed detunings, $\delta = -10$ and $\delta = -50$, and $K = 0 \dots 30$, shown in Fig. 7. For $\delta = -10$, there is a single solution which exists for all K , thus it is not acceptable as a solution. For $\delta = -50$, there are two solutions. The lower one exists in the limit $K \rightarrow \infty$, so it is not acceptable. For the true ground state we then take the other solution that exists in the limit $K \rightarrow 0$. At the critical detuning $\delta_c \simeq -17.8$, the number of solutions switches from one (one physical and one not) to zero (one non-physical).

The fact that f_{GS}^1 only partially separates the all-atom state from a mixed or atom-molecule state is illustrated in Fig. 8. We observe a smooth decrease of the fraction and the half-size of the atomic distribution by increasing K from 0 to 15 at a fixed $\delta = -5$.

We plot the analytical values for f_{GS}^1 based on our variational approximation in Fig. 9. The tip of the fracture occurs for $\delta \approx -17.8$ and $K \approx 13.5$.

To determine the position of the fracture numerically for a fixed δ , we have covered the parameter K in in-

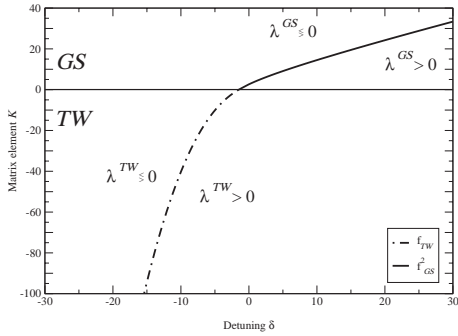


FIG. 10: Outline of the variational solutions of $\lambda^{GS} = 0$ and $\lambda^{TW} = 0$. In regions $\lambda > 0$, there is no solution for the variational size s . In regions where $\lambda \geq 0$ there are two solutions for the variational size s . Fractures f_{TW} and f_{GS}^2 appear as the boundaries between the regions.

δ	K_{th}	K_{num}	N_a^{mix}	$R_{1/2}^{mix}$
-1.5	0	0	-	-
0	2.6	2.5 ± 0.5	0.13	0.76
1	4.1	4.5 ± 0.5	0.18	0.76
5	9.1	9.5 ± 0.5	0.25	0.52
10	14.5	14.5 ± 0.5	0.42	0.28
20	24.2	24.5 ± 0.5	0.55	0.09
30	33.4	33.5 ± 0.5	0.66	0.03

TABLE II: Analytically (K_{th}) and numerically (K_{num}) calculated fracture f_{GS}^2 in the $\{\delta, K\}$ parameter space. The fraction of atoms and the size of the atomic distribution are given for the mixed or atom-molecule state (superscript *mix*) at $K = K_{num} + 0.5$.

crements of 1, and assigned each K to one of the local eigenstates. In this manner we find the position of the fracture line to within ± 0.5 . In Table I we compare the position of the fracture found directly numerically, and analytically using the variational method. The agreement is very good.

In Table I we also report the fraction of atoms and the half-size of the atomic distribution for the two adjacent values of K that we have assigned to different local eigenstates. For instance, the half-size of the atomic distribution on the mixed or atom-molecule side of the fracture decreases when moving away from the origin. This change in size goes from $R_{1/2}^{mix} = 0.33$ at $\delta = -20$ to $R_{1/2}^{mix} = 0.05$ at $\delta = -100$, and more. While in AM-BEC there is no formal collapse of the amplitudes, for large negative values of δ the substantial decrease in the half-size across f_{GS}^1 can convincingly mimic a collapse.

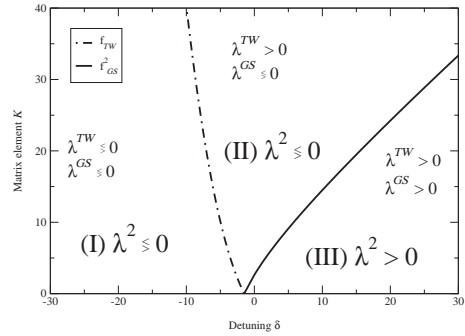


FIG. 11: Regions of λ^2 , Eq.(28), in the parameter space. λ^2 is positive only in Region III, bounded by f_{GS}^2 , for all variational atomic sizes s . In all other regions there exist unstable variational solutions for s , for which $\lambda^2 < 0$.

B. All-molecule state; fractures f_{GS}^2 and f_{TW}

The all-molecule state is the trivial global eigenstate of the AMBEC (3). Numerics shows that the all-molecule state is part of the ground state, and strongly influences the twin state. We analyze the all-molecule state from the perspective of the existence and stability of infinitesimal atomic configurations.

The amplitude of the all-molecule state is simply the ground state wave function of the molecular harmonic potential,

$$\psi(r) = \left(\frac{2m\omega}{\pi}\right)^{3/4} e^{-m\omega r^2}, \quad (19)$$

where m is the mass of the atom and ω is the trapping frequency. The norm of the molecular amplitude is unity, in accord with the all-molecule hypothesis, and the eigenenergy is

$$\mu = \frac{1}{2} \left(\frac{3}{2} - \delta\right). \quad (20)$$

We now analyze the presence of atoms in a perturbative fashion.

1. Existence of variational solutions for the atoms

In the all-molecule approximation an infinitesimal fraction of atoms is roughly described by Eq. (3a), where

$$\mu\varphi = H_a\varphi - K\varphi^*\psi. \quad (21)$$

Here, for the atomic amplitude φ we use the variational expression from Eq. (18), with the size s as the variational parameter. In (21), the eigenenergy μ is given by Eq. (20). Let us introduce a new quantity $\lambda^{GS}(s)$,

$$\lambda^{GS}(s) = \langle\varphi|H_a|\varphi\rangle - \mu - K\langle\varphi^2|\psi\rangle, \quad (22)$$

δ_{th}	K_{th}	δ^{in}	N_a^{in}
-1.5	0	-	-
-3.54	5	-	-
-4.98	10	-3.0	0.21
-7.07	20	-3.9	0.32
-8.66	30	-	-
-11.11	50	-	-
-15.42	100	-	-

TABLE III: Position of f_{TW} in parameter space in the variational approximation. The position of the instability observed in the numerical simulations for a given K is shown in column δ^{in} . In column N_a^{in} is the calculated fraction of the atoms prior to parametric excitations.

in terms of which the Eq. (21) becomes

$$\lambda^{GS}(s) = 0. \quad (23)$$

In the expressions above the actual fraction of atoms cancels out, so the norm of φ can be assumed to be 1. Analysis of the real positive roots of Eq. (23) shows that there are two regions in parameter space, a mixed or atom-molecule region ($\lambda^{GS} \gtrless 0$), in which there are two variational solutions for s , and the all-molecule region, in which there are no such solutions ($\lambda^{GS} > 0$). The fracture f_{GS}^2 is the boundary between the two. This is shown in Fig. 10.

This approach is easily modified to account for the all-molecule part of the twin state. From the zero-mode case, Eq. (10), it follows that in the twin state the phase shift between the molecular amplitude ψ and the matrix element K is -1 . Allowing K to be negative (initially we said that K is non-negative) in Eq. (22) is a way to analyze the all-molecule state of the twin state. Again, we introduce a new quantity, λ^{TW} ,

$$\lambda^{TW} = \langle \varphi | H_a | \varphi \rangle - \mu + K \langle \varphi^2 | \psi \rangle. \quad (24)$$

The variational size of the atoms s is the real positive solution of the equation

$$\lambda^{TW}(s) = 0. \quad (25)$$

We perform the analysis of the real positive roots of Eq. (25), and find a behavior similar to the ground state. In the parameter space of the twin state there are two regions, the all-molecule region, in which there are two variational solutions for s ($\lambda^{TW} \gtrless 0$), and the mixed or atom-molecule region, in which there are no such solutions ($\lambda^{TW} > 0$). This classification is motivated by the numerical results, and is the opposite from the classification for the ground state given above. Nonetheless, the fracture f^{TW} is the boundary between the two regions, as was the case in the ground state. Both fractures and the outline of the properties of the variational solutions are shown in Fig. 10.

In Table II we compare the positions of the fracture f_{GS}^2 found numerically (K_{num}) and analytically (K_{th}),

for various detunings δ . Additionally, the table contains the fraction (N_a^{mix}) and the half-size ($R_{1/2}^{mix}$) of the atomic distribution on the mixed or atom-molecule side of the fracture. Table II indicates that at f_{GS}^2 the two different local eigenstates, the all-molecule state and the mixed or atom-molecule state have the same (lowest) eigenenergy, but do not merge in terms of their properties (size, fraction, etc.). In Table III we compare the position of f_{TW} in the parameter space calculated using the properties of the variational solutions, Eq. (25), and the results from numerical simulations regarding the onset of parametric excitations. Numerical results are limited to two detunings, where for $K = 10, 20$ we find the detuning (δ^{in}) and the fraction of atoms (N_a^{in}) at the onset of the instability.

We note that the analytical results for the all-molecule state differ from the (exact) numerical results in an important aspect. Figs. 4 and 6 show the parametric excitations of the atomic amplitudes in the ground state and the twin state, respectively. In the ground state, a small atomic fraction survives the parametric excitation following f_{GS}^2 , even though there are no available variational atomic configurations ($\lambda^{GS} > 0$). Conversely, the atomic fraction grows exponentially in what is supposed to be the all-molecule region of the twin state, although there are available variational atomic configurations ($\lambda^{TW} \gtrless 0$). We resolve this peculiar behavior by doing the stability analysis of the all-molecule state in the parameter space

2. Stability of the all-molecule state

The starting point for the stability analysis of the all-molecule state is the equation governing the behavior of the atoms, Eq. (3a). Let us write its solution in the form

$$\varphi(\tau) = (a(\tau) + i b(\tau)) \varphi \exp(-i\mu\tau), \quad (26)$$

where φ is the variational atomic amplitude, Eq. (18), and μ is the eigenenergy of the all-molecule state, Eq. (20). Here we assume that the time dependent real functions $a(\tau)$ and $b(\tau)$ are infinitesimals. We use this Ansatz in Eq. (21), multiply both sides with φ^* and integrate in space. In this approximation Eq. (3a) is reduced to a system of ODE for a pair of real functions a and b ,

$$\begin{aligned} \dot{a} &= (\langle \varphi | H_a | \varphi \rangle - \mu + K \langle \varphi^2 | \psi \rangle) b, \\ \dot{b} &= -(\langle \varphi | H_a | \varphi \rangle - \mu - K \langle \varphi^2 | \psi \rangle) a. \end{aligned} \quad (27)$$

We find the characteristic frequency of (27) to be

$$\begin{aligned} \lambda^2(s) &= (\langle \varphi | H_a | \varphi \rangle - \mu)^2 - K^2 |\langle \varphi^2 | \psi \rangle|^2 \\ &= \lambda^{GS}(s) \cdot \lambda^{TW}(s). \end{aligned} \quad (28)$$

As long as $\lambda^2(s) > 0, \forall s > 0$, a small perturbation of the all-molecule state oscillates harmonically; and conversely, if $\exists s' > 0 : \lambda^2(s') < 0$, a deviation from the variational solution begins to grow exponentially.

The characteristic frequency is a product of two terms, λ^{GS} and λ^{TW} . The outline of their variational solutions in the parameter space has been given above and in Fig. 10. However, to have both fractures in the same half of the parameter space ($K > 0$), the fracture f_{TW} needs to undergo a reflection with respect to the $K = 0$ axis ($K \rightarrow -K$). This told, in regard to Eq. (28) the parameter space is divided into three regions (I,II,III) separated by the fractures f_{GS}^2 and f_{TW} , as shown in Fig. 11. In Region I, $\lambda^2(s) = 0$ has 4 real positive solutions, so there are unstable atomic configurations. This region is bounded by f_{TW} . In Region II, bounded by f_{TW} and f_{GS}^2 , $\lambda^2(s) = 0$ has two real positive solutions, so there are unstable atomic configurations as well. It is only in Region III that $\lambda^2(s) > 0, \forall s > 0$. In that part of the parameter space the all-molecule state is stable. Region I is what we call the all-molecule region of the twin state, while Region III is the all-molecule region of the ground state.

We are now able to qualitatively describe the effect of an adiabatic sweep of the detuning on the ground and twin states. In a positive detuning sweep of the ground state, Fig. 4, the fraction of molecules increases while approaching the fracture f_{GS}^2 . Somewhere in the vicinity of f_{GS}^2 the mixed or atom-molecule state disappears and the only available close eigenstate is the all-molecule state. Disappearance of one eigenstate sets on the parametric excitations. The excitations manifests in non-periodic oscillations which are stable, because, as the stability analysis shows, the all-molecule state is stable in this region. However, because the atoms do not have an available variational size s , the shape of the atomic amplitude varies erratically in time. These variations are evident in oscillations of the half-size of the atomic distribution, Fig. 4.

The dynamics of the twin state under the negative detuning sweep follows a similar path prior to f_{TW} , as shown in Fig. 6. The fraction of molecules starts increasing toward f_{TW} , and somewhere close to the fracture the mixed or atom-molecule state disappears. At that point the only nearby eigenstate is the all-molecule eigenstate. However, because the all-molecule state is not stable in this part of the parameter space, the molecules start to decay into atoms. In the numerical simulations we did not find evidence for any other stable eigenstate for the system could settle in. The final result is chaotic oscillations of the AMBEC amplitudes in both shape and fraction.

VI. ABOUT THE EIGENSTATES

In the previous section we calculated the boundaries of the local eigenstates by making use of their properties in the parameter space. We now reorganize these results into a description of the ‘‘global’’ eigenstates, the twin state and the ground state, to which the local eigenstates belong.

A. Ground state

The results of our discussion of the fractures in the ground state are compiled in Fig. 12, which shows the outline of the ground state in the parameter space. The ground state consists of two local eigenstates, the mixed or atom-molecule state and the all-molecule state, separated completely by f_{GS}^2 . Further, the mixed or atom-molecule eigenstate is partially separated from what we call an all-atom state by the fracture f_{GS}^1 . The cut f_{GS}^1 starts at $\delta \simeq -17.8\omega$ and $K \simeq 13.7\omega$. For comparison, on the same figure we give the single GPE collapse boundary, $\frac{K^2}{4\pi\delta} = -0.67\omega$. We conclude that in the ground state the fracture lines correspond to the degeneracy points in the parameter space where two configurations happen to have the same (lowest) total energy.

In a simple AMBEC there is no formal collapse like the one that exists in a single GPE. The formal collapse is prevented by the two-atom resonance term in Eq. (16), which effectively counteracts the scattering term. In Table I we gave the fraction and the half-size of the atomic distribution along f_{GS}^1 calculated numerically on both sides of the fracture for various values of the detuning. We saw a substantial decrease in the half-size of the atomic distribution across the fracture as one moves away from the origin, which may imitate a collapse as observed in a single GPE. In an AMBEC the collapse of the ground state becomes a controllable feature. We may create the collapse by driving the system across f_{GS}^1 , or we may drive the system around the fracture. The latter case should allow, we speculate, creation of a mixed or atom-molecule state of desired size in a continuous fashion and without any parametric excitations.

B. Twin-State

The twin state with its local eigenstates is shown in Fig. 13. The position of the fracture f_{TW} is deduced from f_{GS}^2 by extending the definition of f_{GS}^2 to negative values of K . In the vicinity of f_{TW} (shaded region in Fig. 13) the mixed or atom-molecule state of the twin state disappears. As the nearby all-molecule eigenstate is unstable, the twin state decays rapidly after crossing the fracture. For that reason a conversion of atoms to molecules cannot take place in the twin state. In our numerical simulations we occasionally (not shown in this paper) observed a sequence of parametric excitations resembling a staircase in the shaded region. It appears as if the system went through a series of local eigenstates. However, we have not been able to develop a quantitative characterization of such states, if any.

VII. DISCUSSION

We have studied the eigenstates of the simple atom-molecule Bose-Einstein Condensate both numerically

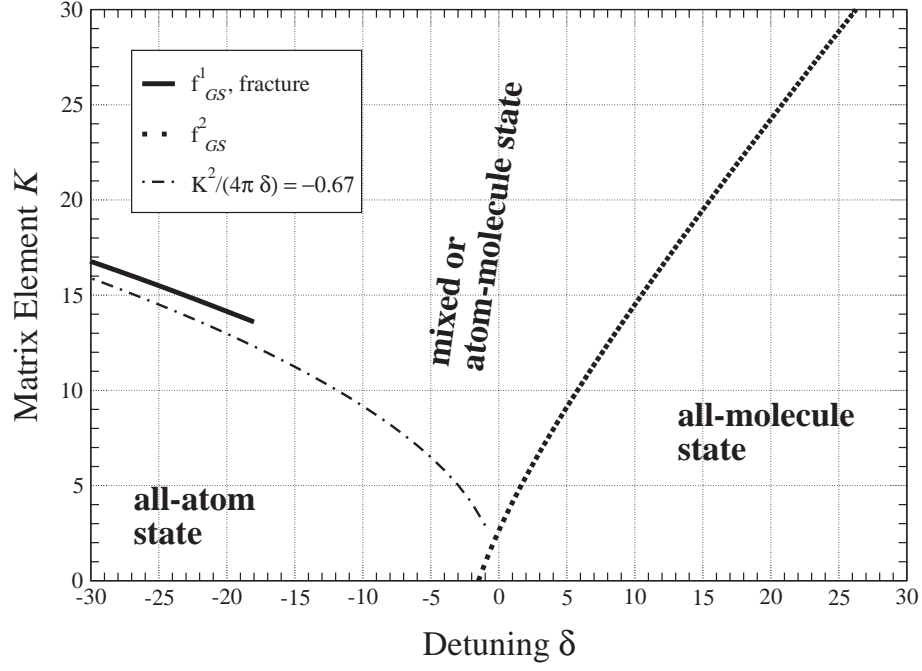


FIG. 12: Map of the ground state with the fractures f_{GS}^1 and f_{GS}^2 separating the three participating eigenstates.

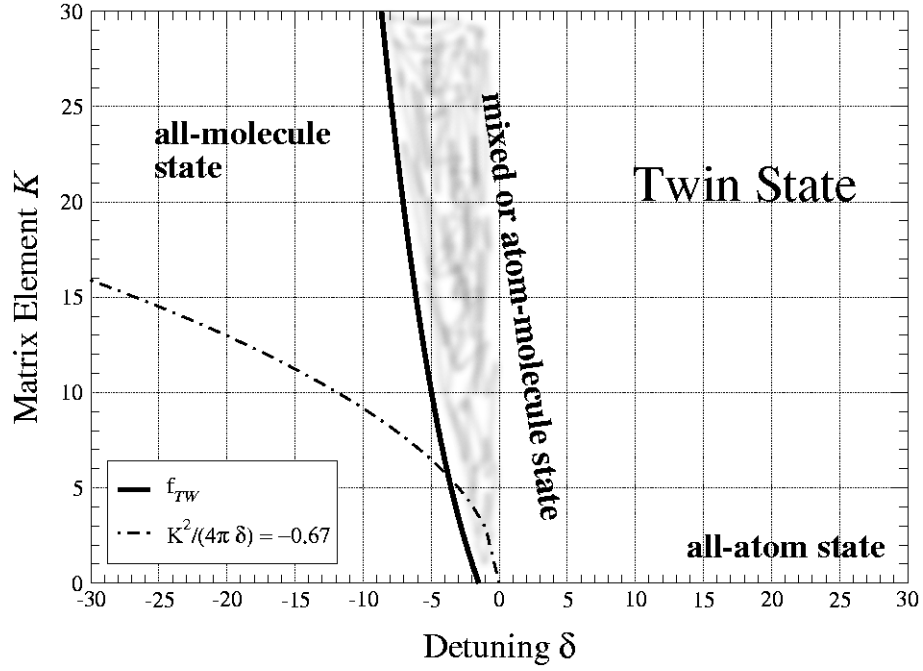


FIG. 13: Map of the twin state with the fracture f_{TW} separating the all-molecule state from the mixed or atom-molecule state. For non-infinitesimal fractions of the atoms, the onset of the instability occurs somewhere in the shaded region.

and analytically. Technically, we are investigating eigenstates of a nonlinear differential operator. The problem proves much trickier than analysis of eigenstates of linear operators. To meet the challenge, we have devised the local eigenstate paradigm. The nature of a global eigenstate is qualitatively different in different regions of the problem parameters, and the transition from one type of local eigenstate to another is typically nonanalytic when a boundary between local eigenstates, a fracture, is crossed. When the problem parameters are varied in time across a fracture, the system will respond to the nonanalyticity with breakdown of adiabaticity and parametric excitations.

Two types of parametric excitations have been encountered. First, the atomic condensate may start to oscillate erratically in shape while maintaining a more or less constant norm (ground state near f_{GS}^2). Second, the atomic condensate may degrade into seemingly chaotic behavior both in shape and in norm (twin state near f_{TW}). In fact, a parameter sweep across the fracture f_{TW} is what is going on in the ‘‘Bosenova’’ experiments [30], and the ensuing loss of the atomic condensate makes a tempting parallel to the chaotic behavior we are predicting. As far as we can tell, in this particular experiment our picture of parametric excitations is as good as any theoretical description of the Bosenova offered to date [7, 31–33].

However, for reasons of time scales, the present approach cannot be the panacea for all of the existing experiments. We are dealing with stationary or near-stationary states of atoms and molecules in a trap, so the trap frequency is a crucial parameter in our calculations. In contrast, say, the Ramsey fringe experiments in an atom-molecule condensate [30] probe time scales orders of magnitude shorter than the time of a back-and-forth oscillation of an atom in the trap. The trap frequency cannot be a significant factor in these experiments. Also, while the chaotic decay of the atomic condensate after a sweep across f_{TW} is reminiscent of both modulational instability of an AMBEC [34] and the phenomenon we [35] have dubbed rogue dissociation, the discussions in Refs. [35–37] are for free atoms. The (likely nontrivial) connection between free and harmonically trapped gases remains to be worked out.

Even though in the present experiments on AMBEC at least the atoms are usually trapped, often the trap is actually irrelevant in the dynamics. In contrast, we have argued that, in a trap, it might be possibly in principle to manipulate a condensate around the fracture f_{GS}^1 , and thereby create a collapsed state of the atom-molecule condensate smoothly and in a completely controllable manner. Studies of a trapped AMBEC on the time scale of the trap, both experimental and theoretical, might have other such intriguing surprises in store.

Acknowledgments

This work is supported in part by NSF (PHY-0097974) and NASA (NAG8-1428).

APPENDIX A: NUMERICS

All numerical calculations in this paper were performed using the novel DS-method [26] which we developed to integrate systems of nonlinear Schrödinger equations such as Eqs. (3). We use pointwise representation for the amplitudes and the operators, with $N = 1024$ being the total number of points and $R_0 = 11$ the spatial extent of the system. The harmonic potential of the trap is isotropic with $\omega = 1$. The trap Hamiltonians H_a and H_m contain only the s-wave parts,

$$H_{a,m}\Phi = -\frac{1}{2m_{a,m}}\frac{d}{dr}\left(r^2\frac{d}{dr}\Phi\right) + \frac{m_{a,m}r^2}{2}\Phi, \quad (\text{A1})$$

where $m_a = 1$ and $m_m = 2$ are the atomic and molecular masses. Integration is performed with a fixed time step chosen according to the prescription

$$\Delta t = \frac{0.01}{\max\left[1, \sqrt{\max_t K(t)}, \max_t |\delta(t)|\right]}. \quad (\text{A2})$$

In each step of the integration in complex time some loss of the norm of the atomic and molecular amplitudes occurs. The renormalization scheme we used to compensate for the losses consists of the following formulae

$$\begin{aligned} \varphi(i\tau + i\Delta\tau) &\rightarrow \sqrt{\frac{1+n_m}{2n_m+n_a}} \cdot \varphi(i\tau + i\Delta\tau), \\ \psi(i\tau + i\Delta\tau) &\rightarrow \sqrt{\frac{2-n_a}{2n_m+n_a}} \cdot \psi(i\tau + i\Delta\tau). \end{aligned} \quad (\text{A3})$$

Here $n_a = \langle \varphi(i\tau + i\Delta\tau) | \varphi(i\tau + i\Delta\tau) \rangle$ and $n_m = \langle \psi(i\tau + i\Delta\tau) | \psi(i\tau + i\Delta\tau) \rangle$ are the norms of the atomic and molecular amplitudes before renormalization. This renormalization furnishes a fixed point with φ and ψ correct to first order in the integration time step Δt . When integrating in real time, the amplitudes φ and ψ may also gradually lose norm. In that case they are renormalized according to the same prescription, Eq. (A3). Half-size of the atomic distribution φ is a numerical solution $R_{1/2}$ of the following equation,

$$\frac{\int_0^{R_{1/2}} dr r^2 |\varphi(r)|^2}{\int_0^\infty dr r^2 |\varphi(r)|^2} = \frac{1}{2}. \quad (\text{A4})$$

We use Eq. (A4) to estimate the extent of the condensate in the trap, and in particular to study the oscillations the condensate may undergo following the parametric excitation at a fracture.

-
- [1] E. Gross, *Nuovo Cimento* **20**, 454 (1961).
- [2] L. Pitaevskii, *Zh. Eksp. Teor. Fiz.* **40**, 646 (1961), english translation in *Sov. Phys. JETP* **13**, 451 (1961).
- [3] F. Dalfovo and S. Stringari, *Phys. Rev. A* **53**, 2477 (1996).
- [4] R. Duine and H. T. C. Stoof, *Explosion of a Collapsing Bose-Einstein Condensate* (2001).
- [5] J. M. Gerton, D. Strekalov, I. Prodan, and R. G. Hulet, *Nature* **408**, 692 (2000).
- [6] E. Donley, N. Claussen, S. Cornish, J. Roberts, E. Cornell, and C. Wieman, *Nature* **412**, 295 (2001).
- [7] R. Duine and H. Stoof, *J. Opt. B* **5**, 212 (2003).
- [8] M. Wadati and T. Tsurumi, *Phys. Lett. A* **247**, 287 (1998).
- [9] H. Stoof, *Phys. Rev. A* **49**, 3824 (1994).
- [10] E. Timmermans, P. Tommasini, R. Côté, M. Hussein, and A. Kernan, *Phys. Rev. Lett.* **83**, 2691 (1999).
- [11] S. Koh, *Phys. Rev. B* **64**, 134529 (2001).
- [12] S. Cornish, N. Claussen, J. Roberts, E. Cornell, and C. Wieman, *Phys. Rev. Lett.* **85**, 1795 (2000).
- [13] S. Kokkelmans, J. Milstein, M. Chiofalo, R. Walser, and M. Holland, *Phys. Rev. A* **65**, 53617 (2002).
- [14] T. Weber, J. Herbig, M. Mark, H. Nagerl, and R. Grimm, *Science* **299**, 232 (2003).
- [15] E. Timmermans, P. Tommasini, M. Hussein, and A. Kernan, *Phys. Rep.* **315**, 199 (1999).
- [16] P. O. Fedichev, Y. Kagan, G. V. Shlyapnikov, and J. T. M. Walraven, *Phys. Rev. Lett.* **77**, 2913 (1996).
- [17] J. Bohn and P. Julienne, *Phys. Rev. A* **60**, 414 (1999).
- [18] M. Koštrun, M. Mackie, R. Côté, and J. Javanainen, *Phys. Rev. A* **62**, 063616 (2000).
- [19] J. Roberts, N. Clausen, S. Cornish, E. Donley, E. Cornell, and C. Wieman, *Phys. Rev. Lett.* **86**, 4211 (2001).
- [20] D. Kaplan, M. Savage, and M. Wise, *Nucl. Phys. B* **478**, 629 (1996).
- [21] E. Tiesinga, B. Verhaar, and H. Stoof, *Phys. Rev. A* **47**, 411 (1993).
- [22] J. P. Burke, C. H. Greene, and J. L. Bohn, *Phys. Rev. Lett.* **81**, 3355 (1998).
- [23] M. Marinescu and L. You, *Phys. Rev. Lett.* **81**, 4596 (1998).
- [24] A. Derevianko, W. R. Johnson, M. S. Safronova, and J. F. Babb, *Phys. Rev. Lett.* **82**, 3589 (1999).
- [25] Y. Wu and R. Côté, *Phys. Rev. A* **65**, 053603 (2002).
- [26] M. Koštrun and J. Javanainen, *J. Comp. Phys.* **172**, 298 (2001).
- [27] M. Koštrun and J. Javanainen, *Phys. Rev. A* **65**, R031602 (2002).
- [28] F. Dalfovo, S. Georgini, L. Pitaevskii, and S. Stringari, *Rev. of Mod. Phys.* **71**, 463 (1999).
- [29] A. Parkins and D. Walls, *Phys. Rep.* **303**, 1 (1998).
- [30] E. Donley, N. Claussen, S. Thompson, and C. Wieman, *Nature* **417**, 529 (2002).
- [31] M. Mackie, K.-A. Suominen, and J. Javanainen, *Phys. Rev. Lett.* **89**, 180403 (2002).
- [32] S. Kokkelmans and M. Holland, *Phys. Rev. Lett.* **89**, 180401 (2002).
- [33] T. Köhler, T. Gasenzer, and K. Burnett, *Phys. Rev. A* **67**, 013601 (2003).
- [34] J. Javanainen and M. Koštrun, *Optics Express* **5**, 188 (1999).
- [35] J. Javanainen and M. Mackie, *Phys. Rev. Lett.* **88**, 090403 (2002).
- [36] K. Goral, M. Gajda, and K. Rzazewski, *Phys. Rev. Lett.* **86**, 1397 (2001).
- [37] M. Holland, J. Park, and R. Walser, *Phys. Rev. Lett.* **86**, 1915 (2001).